Available online at www.sciencedirect.com

SciVerse ScienceDirect

Ceramics International 38 (2012) 6303–6310

CERAMICS INTERNATIONAL

www.elsevier.com/locate/ceramint

A bi-layer cathode based on lanthanum based cobalt- and iron-containing perovskite and gadolinium doped ceria for thin yttria stabilized zirconia electrolyte solid oxide fuel cells

Ju Hee Kim[a], Yong-il Park[b], Haekyoung Kim[a,*]

[a]School of Materials Science & Engineering, Yeungnam University, Gyeongsan 712-749, Republic of Korea
[b]School of Materials & System Engineering, Kumoh National Institute of Technology, Gumi 730-701, Republic of Korea

Received 20 February 2012; received in revised form 28 April 2012; accepted 30 April 2012
Available online 11 May 2012

Abstract

Composite cathodes based on $La_{0.6}Sr_{0.4}Co_{0.2}Fe_{0.8}O_{3-\delta}$ (LSCF) are investigated for lower operating temperature ($<750\,^{\circ}C$) applications of a solid oxide fuel cell (SOFC). To enhance a charge transfer, a bi-layer SOFC cathode is proposed, which has a LSCF–$Ce_{0.9}Gd_{0.1}O_{1.95}$ (GDC) composite layer and a pure LSCF layer. The bi-layer cathode SOFC shows a current density of 0.65 A cm^{-2} at 0.8 V and 660 °C, which is higher than a LSCF–GDC composite single-layer cathode SOFC cell of 0.35 A cm^{-2}. The charge transfer polarizations in the bi-layer cathode SOFC are 0.14 Ω cm^2 and 0.35 Ω cm^2 at 760 °C and 660 °C, respectively, which are lower than those in the single-layer cathode cell of 0.23 Ω cm^2 and 0.66 Ω cm^2. The impedances characterized with a fitting model show that the lowered charge transfer polarization in the bi-layer cathode is a dominant factor in reducing the total polarization of SOFC.

Keywords: E. Fuel cells; Electrochemistry; Electrical conductivities; Oxide

1. Introduction

The development of solid oxide fuel cells (SOFCs) for intermediate temperature (IT, 600–800 °C) operations have been considered as the most promising future component related to energy generation for power plants and distributed power systems. For operation at IT, perovskite-based compounds having the general formula of $La_{0.6}Sr_{0.4}Co_{0.2}Fe_{0.8}O_{3-\delta}$ (LSCF) with a Gd-doped ceria (GDC)-based interlayer have been reported to be very effective owing to their high ionic conductivity and catalytic activity [1–6]. In LSCF-based cathodes, electrochemical reactions occur at both the triple phase boundary (LSCF and oxygen gas) and the surface of LSCF. To enhance the ionic conductivity and prevent the coarsening of the cathode, the addition of a second phase such as GDC has been reported and many studies have confirmed that the formation of a composite cathode can beneficially reduce the polarization resistance of a pure LSCF cathode [7–18]. Even if LSCF has a good ionic conductivity, its electronic conductivity is much more relevant for SOFC cathode. So the addition of other materials, such as GDC, which has a high ionic conductivity, is effective in increasing the overall charge transfer of the composite electrode LSCF–GDC. This phenomenon is attributed to the extension of the three-phase boundary (TPB) of the electrolyte (ionic conductor), cathode (electronic conductor) and gas phase (oxygen or air used as an oxidant). Additional benefits include better adhesion and thermal expansion match to the electrolyte layer or interlayer [19]. Composite electrodes commonly containing 40–60 wt% of electrolyte materials are characterized to have low electronic conductivity, which can be resolved using a design of bi-layer electrodes of the cathode functional layer and the current collector layer. The cathode functional layer, which directly contacts the electrolyte, needs to have good thermal and chemical compatibility with the electrolyte and provide high electrochemical activity for oxygen reduction. The outer current collector layer, on the other

*Corresponding author. Tel.: +82 53 810 2536; fax: +82 53 810 4628.
E-mail address: hkkim@ynu.ac.kr (H. Kim).

0272-8842/$36.00
http://dx.doi.org/10.1016/j.ceramint.2012.04.086

hand, is usually composed of high electronic conductive materials to facilitate a uniform current distribution along the cathode and to help the electrons transfer from the outer circuit to the TPB of the cathode functional layer [20]. Similar to bi-layer cathode, multilayer cathode and functionally graded composite cathode are fabricated through inserting layers with different cathode/electrolyte ratios to guarantee a smooth transition from one cathode material to another cathode material [21] or from one electrolyte material to another electrolyte material [22,23]. With the $Sm_{0.2}Ce_{0.8}O_{2-\delta}$ (SDC) as an electrolyte, the addition of SDC to LSCF shows the improvement of the adhesion of the cathode layer to electrolyte layer, and the thickness of the composite layer should be optimized to minimize the ohmic and polarization resistance and maximize the cell performance [24]. This enhanced performance of both a composite and a layered cathode is a function of sintering temperature, microstructure (such as the grain size and porosity), and composition of LSCF and GDC.

In this study, LSCF synthesized via a complex method with an inorganic nano-dispersant is used for cathode, and a bi-layer cathode based on nanocrystalline LSCF is proposed to enhance the electrical conductivity for thin yttrium stabilized zirconia (YSZ) electrolyte SOFCs. The bi-layer cathode includes a LSCF–GDC composite layer and a LSCF layer. LSCF–GDC layer comes into contact with a GDC interlayer and a LSCF layer with a current collector. LSCF layer in the bi-layer cathode is expected to provide higher electronic conductivity than LSCF–GDC composite layer, and is likely to be beneficial for enhancing an electronic transfer. SOFC with the bi-layer cathode electrode is characterized in terms of its fuel cell performance and impedances, and compared with the single-layer cathode SOFC. The performances of SOFC are characterized by the equivalent circuit developed with five RQ (resistance and constant phase in series) and the fitted results are compared with experiment data and the five RQ elements are characterized. The characterized impedances are studied to clarify the effects of the bi-layer cathode design in SOFCs.

2. Experimental procedures

The LSCF cathode materials, with a surface area of $80\ m^2\ g^{-1}$, were synthesized using the method described in a previous work [25]. The GDC materials, with a surface area of $15\ m^2\ g^{-1}$, were purchased from ANAN Kasei. Metal precursors of lanthanum nitrate ($La(NO_3)_3 \cdot 6H_2O$, YAKURI, 97%), strontium nitrate ($Sr(NO_3)_2$, JUNSEI, 97%), cobalt nitrate ($Co(NO_3)_2 \cdot 6H_2O$, JUNSEI, 97%), and ferric nitrate ($Fe(NO_3)_3 \cdot 9H_2O$, JUNSEI, 97%) were used for the LSCF perovskite powders. Ethylenediaminetetraacetic acid powder (YAKURI) and crystallized citric acid (DUKSAN), each with a purity level higher than 99.5%, were used as the raw materials for chelation. As previous work [25], a homogeneous metal nitrate solution was prepared by dissolving lanthanum nitrate, strontium nitrate, cobalt nitrate, and ferric nitrate into a deionized water with a mole ratio of 6:4:2:8. Next, solid citric acid was added to the mixed metal nitrate solution, followed by EDTA powder. The solution was then heated in a water bath at 70 °C until it became clear, at which point 5 g of HI BLACK170 carbon black was added as an inorganic nano-dispersant. The mixture was reheated until a magnetic bar immersed in the solution stopped rotating. The remaining mixture was dried overnight at 80–120 °C in a vacuum oven to remove the residual water. The dried mixture was crushed and calcined at 700 °C for 5 h to form a perovskite phase and to remove any organic compounds and inorganic nano-dispersants.

The anode-supported cells of $32 \times 22\ cm^2$, which consist of Ni-YSZ of 900 μm as a support, Ni-YSZ of 20 μm as an anode functional layer, and YSZ of 10 μm as an electrolyte, were prepared by a tape-casting and co-firing method at 1370 °C for 3 h. GDC of 1 μm as an interlayer was formed onto the YSZ electrolyte by an aerosol deposition method with the carrier gas, compressed air dried through a dehumidifying filter, in the aerosol chamber evacuated using a rotary pump. The anode supported SOFCs were cut into circles with diameters of 2.6 cm from a 32×22 cm plate.

The composite cathodes were prepared with LSCF-based nanocrystalline powders (surface area of $80\ m^2\ g^{-1}$) and GDCs (surface area of $15\ m^2\ g^{-1}$). For preparing LSCF–GDC composite cathode, LSCF and GDC were mixed together in ratios of 50:50 wt% with organic binder solution, ethyl cellulose, and di-ethylene glycol butyl ether with α-terpinol. The bi-layer cathode is fabricated by screen-printing of LSCF–GDC paste on the GDC interlayer followed by the drying in oven at 120 °C. After drying, the LSCF paste is printed and the bi-layer cathode is sintered at 900 °C for 3 h. The thickness of each layer is controlled by the number of prints done. For the bi-layer cathode, a paste with LSCF and GDC was printed twice onto a GDC interlayer and a LSCF paste was then printed once onto the LSCF–GDC composite layer. After printing the LSCF–GDC composite and the LSCF layer, the SOFC was sintered at 900 °C for 3 h. The active cathode area was $0.785\ cm^2$. The SOFC with a single-layer consisted of only a LSCF–GDC composite layer. A paste of LSCF and GDC was printed three times onto a GDC interlayer, followed by drying in oven at 120 °C and sintering at 900 °C for 3 h. The fabricated cells were assembled and sealed with Cerama bond™ 571 from AREMCO in a ceramic jig to measure current–voltage characteristic and impedances. The ceramic jig is shown in Fig. 1. Pt paste and mesh was used for current collecting. The cells were heated to 780 °C in 9 h and the anode reduction was performed with $300\ cc\ min^{-1}$ of 97% H_2–3% H_2O for 3 h. The fuel cell performances and the impedances were characterized and analyzed with 300 cc min^{-1} of 97% H_2–3% H_2O and $1000\ cc\ min^{-1}$ of air. The impedance was measured with the WEIS system from

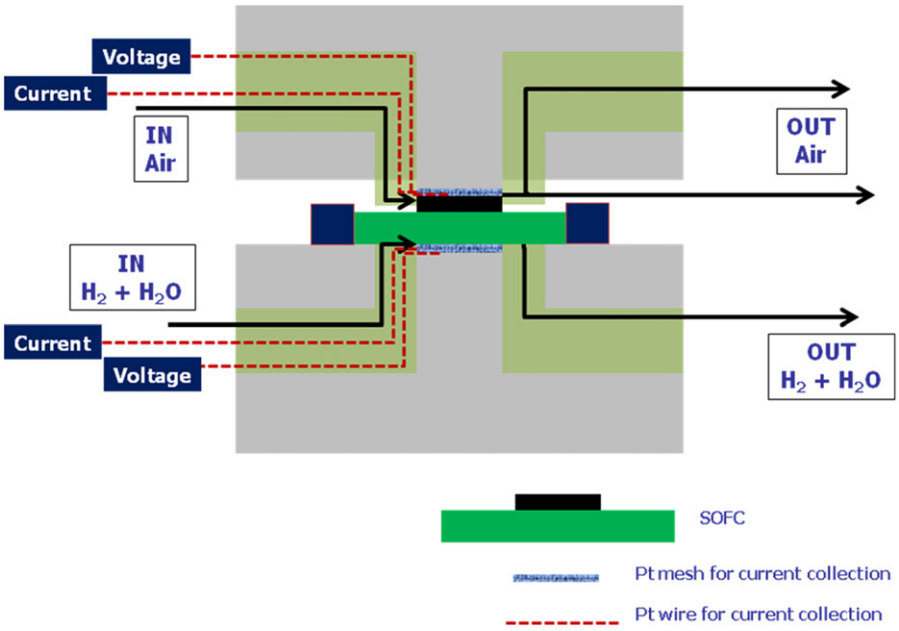

Fig. 1. Schematic diagram of jig for measurements.

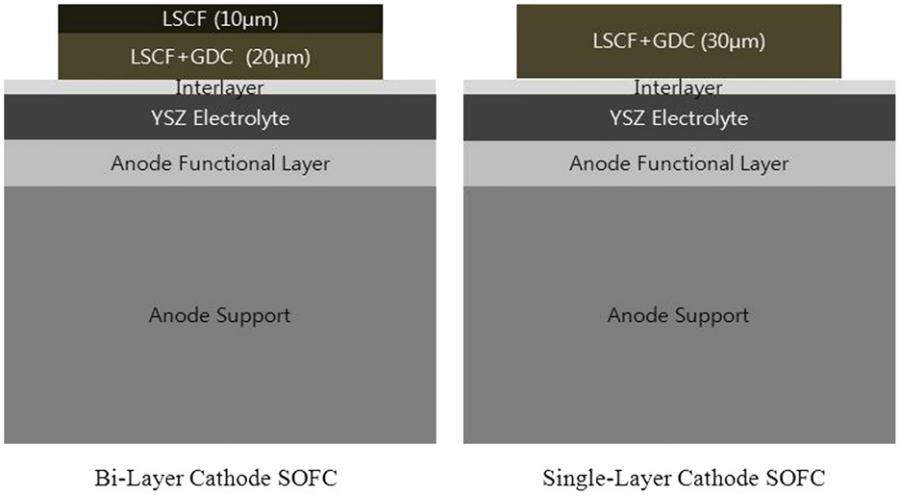

Fig. 2. Schematic diagram of the bi-layer cathode and the single-layer cathode.

WonAtech. The impedance spectra were obtained in the frequency range of 100 kHz–0.1 Hz with applied ac voltage amplitude of 100 mV at cell potential of OCV, 0.9 V, and 0.7 V. After electrochemical measurements, the microstructures of SOFCs were characterized with scanning electron microscopy of JSM-6480LV.

3. Results and discussions

A schematic diagram of the bi-layer cathode and the single-layer cathode is shown in Fig. 2. The bi-layer cathode consists of a LSCF–GDC composite layer of 20 μm and a pure LSCF layer of 10 μm. The single-layer cathode consists of a LSCF–GDC composite layer of 30 μm. The thickness of cathode in both cells is well controlled to have the same value of 30 μm. The cathodes have good contact with a GDC interlayer as shown in the microstructures of Fig. 3. Cerium and lanthanum profiles of cathode layer with energy dispersive spectrometer (EDS) are shown in Fig. 3(b) and (d). Lanthanum and cerium are uniformly distributed in whole cathode area of single-layer cathode cell in Fig. 3(d). In bi-layer cathode SOFC, the distribution of cerium is not uniform and cerium barely exists in the layer contacted with current collector as shown in Fig. 3(b). In the bi-layer cathode, the EDS profiles classify the LSCF–GDC composite layer and the LSCF layer, which show that the bi-layer cathode electrode is successfully fabricated.

The fuel cell performances are characterized with H_2–3% H_2O of 400 cc min^{-1} and air of 1000 cc min^{-1}. Fig. 4

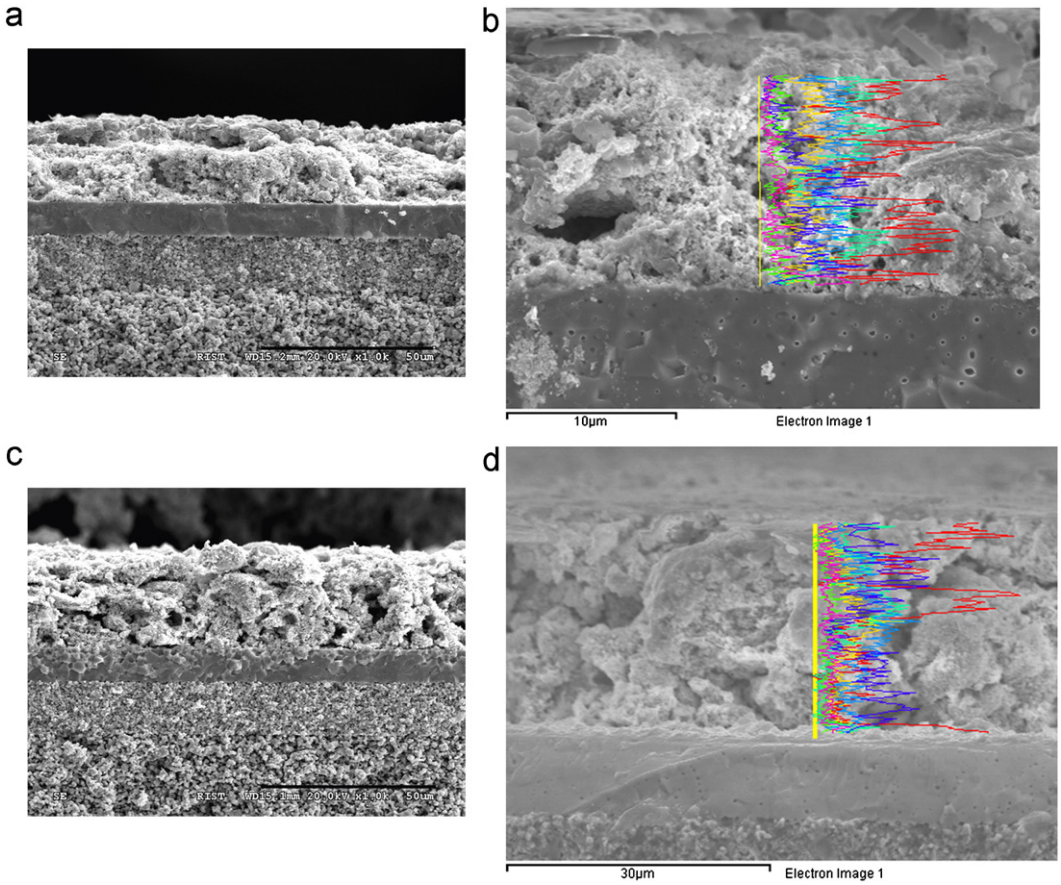

Fig. 3. (a) Cross-sectional image of the bi-layer cathode SOFC. (b) EDS profile of the bi-layer cathode SOFC. (c) Cross-sectional image of the single-layer cathode SOFC. (d) EDS profile of the single-layer cathode SOFC.

shows the fuel cell performances of SOFCs with the bi-layer cathode and the single-layer cathode. The SOFC with the bi-layer cathode at 0.8 V shows current densities of 1.3 A cm^{-2}, 0.97 A cm^{-2}, and 0.65 A cm^{-2}, at 760 °C, 710 °C, and 660 °C, respectively. The maximum power density is over 1.5 W cm^{-2} at 760 °C in the SOFC with the bi-layer cathode. The SOFC with the single-layer cathode at 0.8 V shows the current densities of 1.17 A cm^{-2}, 0.70 A cm^{-2}, and 0.35 A cm^{-2} at 760 °C, 710 °C, and 660 °C, respectively. The current density of the bi-layer cathode cell at 760 °C is 1.1 times higher than that of the single-layer cathode cell. The performance gap between the bi-layer and single-layer cathode SOFC increases as the temperature decrease. For the current density at 660 °C, the fuel cell performance of the bi-layer cathode cell is 1.8 times higher than that of the single-layer cathode cell. The effects of the LSCF layer on enhancing the electronic conductivity in the bi-layer cathode are becoming dominant as the temperature decreases. The higher fuel cell performance of the bi-layer cathode cell results from an enhanced the charge transfer at a lower temperature due to the enhanced electronic transport of the LSCF layer.

The effects of the bi-layer cathode are characterized with the impedances of the SOFCs and the impedances are shown in Fig. 5. The total resistances of the single-layer cathode cell at open circuit voltage (OCV) are 0.60 Ω cm^2, 0.74 Ω cm^2, and 1.15 Ω cm^2 at 760 °C, 710 °C, and 660 °C, respectively. Those of the bi-layer cathode cell at OCV are 0.38 Ω cm^2, 0.48 Ω cm^2, and 0.66 Ω cm^2 at 760 °C, 710 °C, and 660 °C, respectively. The resistances of the SOFC with the bi-layer cathode are lower than those of the single-layer cathode cell. The ohmic resistance of the bi-layer cathode cell is also lower than those of the single-layer cathode cell in all temperature ranges. The impedance values decrease clearly when tested at 0.9 V and 0.7 V. The low-frequency intercept of the impedance spectra shows the areal specific resistance of the cell, and the slope of the current–voltage curve at each voltage is identical to the area specific resistance as measured by impedance measurements. As shown in Fig. 4, a decrease of the slope in the current–voltage curve is observed as the potential decrease from OCV to 0.9 V and 0.7 V.

The impedances of the SOFCs are fitted with an equivalent circuit as shown in Fig. 6. In this study, the electrochemical diagnosis process contains measuring, modeling with equivalent circuit model (ECM), fitting, and interpretation. The ECM is phenomenological and easily accepted and understood, and each discrete circuit element of the ECM is supposed to have corresponding physical and chemical meanings, such as mass-transfer, electron transfer, electrolyte resistance, and electrochemical reaction conductance. AC impedance measurements

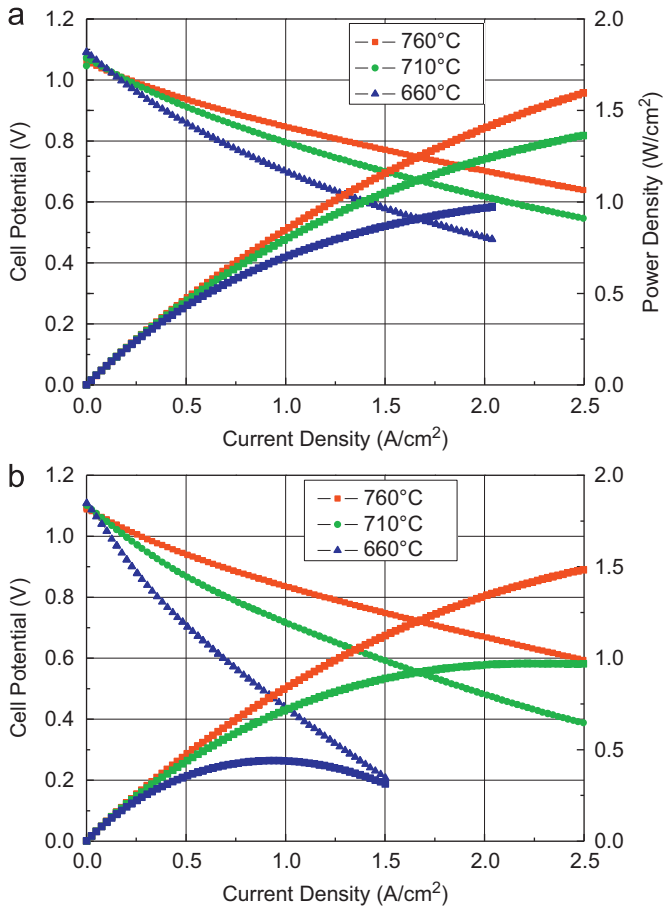

Fig. 4. (a) Fuel cell performances of the bi-layer cathode SOFC. (b) Fuel cell performances of the single-layer cathode SOFC.

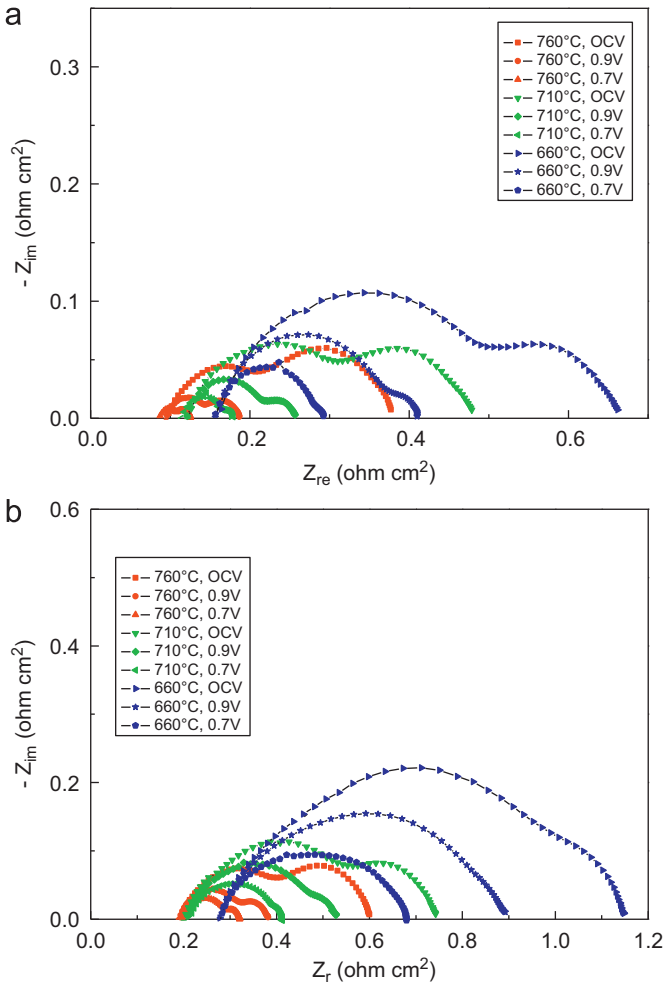

Fig. 5. (a) Impedance of the bi-layer cathode SOFC. (b) Impedance of the single-layer cathode SOFC.

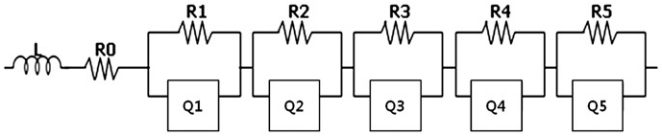

Fig. 6. Equivalent circuits for fitting.

are conducted at a wide range of frequencies from 0.1 Hz to 100 kHz, which allows the analysis of several overlapping of physical and chemical responses. Barfod et al., [26] and Leonide et al. [27,28] present an equivalent circuit of the anode supported SOFC, which has capability to characterize five physicochemical processes in SOFCs [26]. In this study, the impedances are modeled by five RQ elements based on their circuit. The notice of 0 to 5 represents each response to the AC perturbation and it decreases with characteristic frequency. R0 is from the ohmic resistance of an electrolyte, electrodes, and the connection wires, and L is the inductance, which is attributed to the platinum current–voltage probes or the heating elements of the furnace used to heat up the sample. (R1Q1) corresponds to the charge transfer reactions at electrode, which include polarization of the interface between the electrolyte and electrode; (R2Q2) corresponds to the charge transfer reaction and ionic transport coupled with the gas diffusion; (R3Q3) corresponds to the oxygen surface exchange kinetics and oxygen ion diffusivity at the cathode. (R4Q4) and (R5Q5) correspond to the gas diffusion reaction, which are related with the mass transfer reactions at the electrodes [27–29]. Each discrete circuit element can be the coupled with the physical and chemical reactions in SOFCs. The fitting results of the SOFCs at OCV are presented in Fig. 7, which show the excellent matching with experimental results. In the bi-layer cathode cell, the polarizations at the low-frequency ranges are consistent at all temperature ranges, while the polarizations at the high-frequency range decrease with an increase in the temperature as shown in Fig. 7. The polarization of the SOFC with the bi-layer cathode may be reduced due to the enhanced electronic conductivity of the LSCF layer. The charge transfer resistance (the sum of R1, R2, and R3) of the bi-layer cathode cell at 760 °C is 0.14 Ω cm^2, which is lower than that of the single-layer cathode cell, 0.23 Ω cm^2. The charge transfer resistances (the sum of R1, R2, and R3) are the most dominant factor in the reduction of the polarizations in bi-layer cathode, as shown in Fig. 8(a).

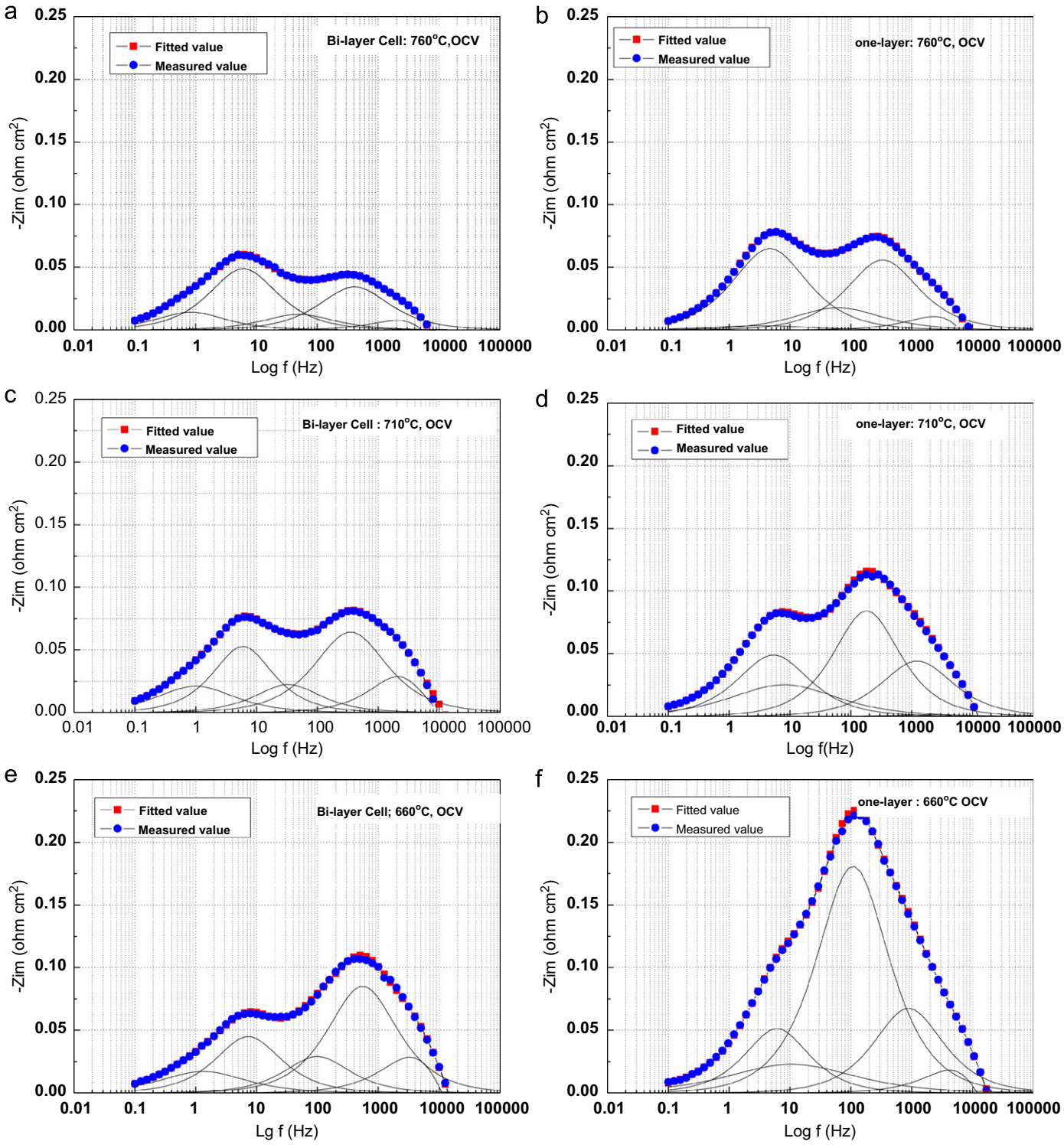

Fig. 7. (a) Impedance of the bi-layer cathode SOFC at 760 °C and OCV. (b) Impedance of the single-layer cathode SOFC at 760 °C and OCV. (c) Impedance of the bi-layer cathode SOFC at 710 °C and OCV. (d) Impedance of the single-layer cathode SOFC at 710 °C and OCV. (e) Impedance of the bi-layer cathode SOFC at 660 °C and OCV. (f) Impedance of the single-layer cathode SOFC at 660 °C and OCV.

As the temperature decrease, the increment of the charge transfer polarization becomes dominant in the single-layer cathode. No significant differences are noted in sum of R4 and R5 among all cases, and the mass transfer polarization is not likely to be affected by the LSCF layer. R1, R2, and R3 values of both cells are compared with temperature, as shown in Fig. 8(b). R3 value is the dominant factor that reduced the polarization in the bi-layer cathode cell. R3 at 760 °C and open circuit voltage is 0.038 $\Omega\,cm^2$ in the bi-layer cathode cell and 0.066 $\Omega\,cm^2$ in the single-layer

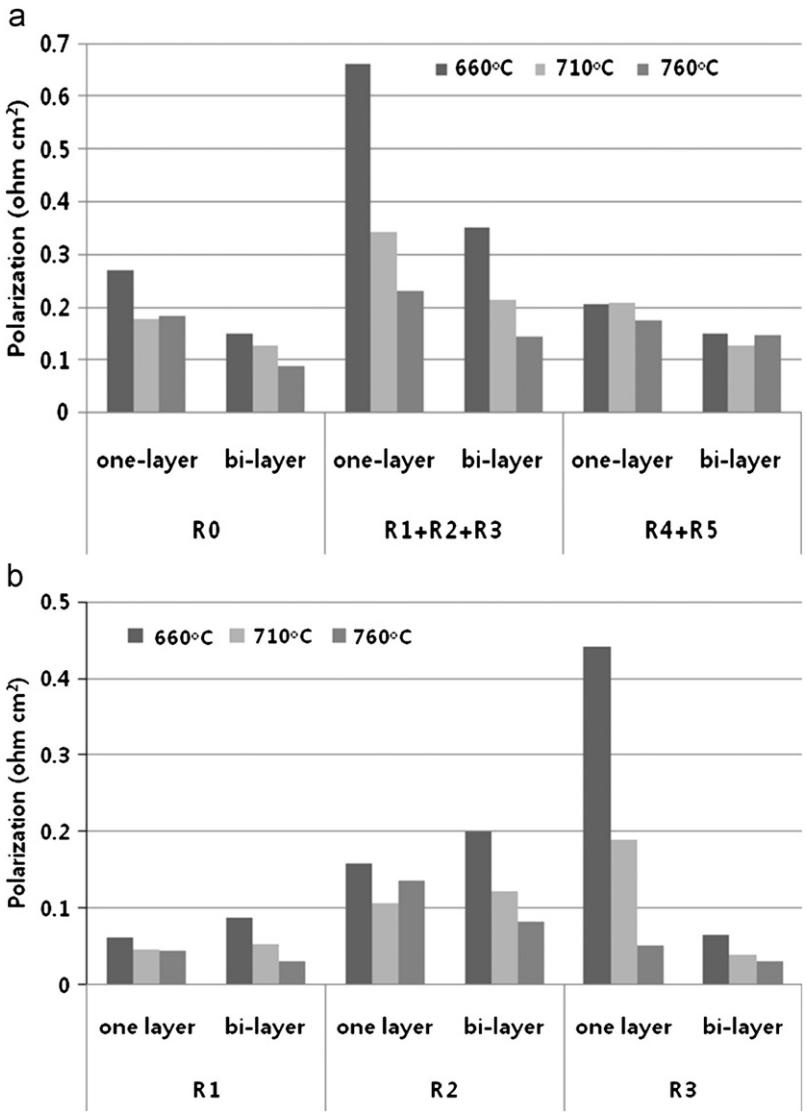

Fig. 8. Fitting results of impedances (a) Total polarization. (b) Charge transfer polarization.

cathode cell. R3 values in the single-layer cathode cell increase dramatically from 0.066 $\Omega\,cm^2$ to 0.56 $\Omega\,cm^2$ as the temperature decrease from 760 °C to 660 °C, while in the bi-layer cathode cell R3 values are 0.038 $\Omega\,cm^2$, 0.05 $\Omega\,cm^2$, and 0.083 $\Omega\,cm^2$, at 760 °C, 710 °C and 660 °C, respectively. From the fitted results, the bi-layer cathode beneficially reduces the charge transfer polarization, which is especially concerned with R3. The enhanced charge transfer of the LSCF layer in the bi-layer cathode leads to higher fuel cell performance, especially when the SOFC operates at a lower temperature. R3 in an equivalent circuit model is expected to concern with the charge transfer reaction of a cathode with a current collector, the oxygen surface exchange kinetics, and oxygen ion diffusivity of a LSCF cathode. However, one RQ element might be related with other reaction from the cathode due to the overlapping of the characteristic frequencies. Much of work should be needed to clarify the relationship among the electrochemical process, measurement variables, and their contribution to the impedance spectra of SOFCs.

4. Conclusions

$La_{0.6}Sr_{0.4}Co_{0.2}Fe_{0.8}O_{3-\delta}$ with a surface area of 80 $m^2\,g^{-1}$ and $Ce_{0.9}Gd_{0.1}O_{1.95}$ (GDC) with a surface area of 15 $m^2\,g^{-1}$ are used as cathode materials for solid oxide fuel cells. A composite cathode with LSCF and GDC is fabricated for a single-layer cathode. To enhance the electrical conduction with a cathode current collector, a LSCF layer is added on the LSCF–GDC composite cathode. A SOFC with the bi-layer cathode shows a current density at 0.8 V of 1.3 A cm^{-2}, 0.97 A cm^{-2}, and 0.65 A cm^{-2} at 760 °C, 710 °C, and 660 °C, respectively. The maximum power density is over 1.5 W cm^{-2} at 760 °C in the SOFC with the bi-layer cathode. The SOFC with the single-layer cathode shows a current density at 0.8 V

of 1.17 A cm^{-2}, 0.70 A cm^{-2}, and 0.35 A cm^{-2}, at 760 °C, 710 °C, and 660 °C, respectively. The impedance of the SOFC with the bi-layer cathode shows much lower polarization due to the enhanced charge transfer. The charge transfer polarizations in the bi-layer cathode cell are 0.14 Ω cm^2 and 0.35 Ω cm^2 at 760 °C and 660 °C, respectively, which are lower than those in the single-layer cathode cell of 0.23 Ω cm^2 and 0.66 Ω cm^2 at 760 °C and 660 °C, respectively. The enhanced charge transfer in the bi-layer cathode leads to higher fuel cell performance, especially when the SOFC operates at a lower temperature. With equivalent circuit model (ECM), the charge transfer polarization, especially R3 elements, is a dominant factor for reducing the polarization of the bi-layer cathode SOFC. Even though R3 elements might be related with other reaction from the cathode due to the overlapping of the characteristic frequencies, it is confirmed that the enhanced fuel cell performance using the bi-layer cathode results from the lowered charge transfer polarization of the cathode.

Acknowledgments

This work was supported by the National Research Foundation of Korea Grant funded by the Korean Government (MEST) (NRF-2011-R1-0009667).

References

[1] S.P. Jiang, A comparison of O_2 reduction reactions on porous (La,Sr)MnO_3 and (La,Sr)(Co,Fe)O_3 electrodes, Solid State Ionics 146 (2002) 1–22.
[2] M.J. Jørgensen, M. Mogensen, Tape cast solid oxide fuel cell LSM/YSZ composite cathodes, Journal of the Electrochemical Society 148 (2001) A433–442.
[3] V. Dusastre, J.A. Kilner, Optimisation of composite cathodes for intermediate temperature SOFC applications, Solid State Ionics 126 (1999) 163–174.
[4] D. Kusscer, J. Holc, S. Hrovat, D. Kolar, Correlation between the defect structure, conductivity and chemical stability of $La_{1-y}Sr_yFe_{1-x}Al_xO_{3-\delta}$ cathodes for SOFC, Journal of the European Ceramic Society 211 (2001) 1817–1820.
[5] A. Mai, V. Haanappel, S. Uhlenbruck, F. Tietz, D. Stöver, Ferrite-based perovskites as cathode materials for anode-supported solid oxide fuel cells: part I variation of composition, Solid State Ionics 176 (2005) 1341–1350.
[6] A. Mai, V. Haanappel, S. Uhlenbruck, F. Tietz, D. Stöver, Solid State Ionics 177 (2006) 2103.
[7] Y. Teraoka, H.M. Zhang, K. Okamoto, N. Yamazoe, Recent advances in single-chamber fuel-cells: experiment and modeling, Materials Research Bulletin 23 (1988) 51–58.
[8] J. Fleig, On the width of the electrochemically active region in mixed conducting solid oxide fuel cell cathodes, Journal of Power Sources 105 (2002) 228–238.
[9] V.A.C. Haanappel, J. Mertens, D. Rutenbeck, C. Tropartz, W. Herzhof, D. Sebold, F. Tietz, Optimisation of processing and microstructural parameters of LSM cathodes to improve the electrochemical performance of anode-supported SOFCs, Journal of Power Sources 141 (2005) 216–226.
[10] S.B. Adler, J.A. Lane, B.C.H. Steele, Electrode kinetics of porous mixed-conducting oxygen electrodes, Journal of the Electrochemical Society 143 (1996) 3554–3564.
[11] J.A. Kilner, R.A. De Souza, I.C. Fullarton, Surface exchange of oxygen in mixed conducting perovskite oxides, Solid State Ionics 86–88 (1996) 703–709.
[12] J. Fleig, Solid oxide fuel cell cathodes: polarization mechanisms and modeling of the electrochemical performance, Annual Review of Materials Research 33 (2003) 361–382.
[13] V. Srdic, R.P. Omorjan, J. Seidel, Electrochemical performances of (La,Sr)CoO_3 cathode for zirconia-based solid oxide fuel cells, Materials Science and Engineering B 116 (2005) 119–124.
[14] E.P. Murray, M.J. Sever, S.A. Barnett, Electrochemical performance of (La,Sr)(Co,Fe)O_3–(Ce,Gd)O_3 composite cathodes, Solid State Ionics 148 (2002) 27–34.
[15] N. Gunasekaran, S. Saddawi, J.J. Carberry, Effect of surface area on the oxidation of methane over solid oxide solution catalyst $La_{0.8}Sr_{0.2}MnO_3$, Journal of Catalysis 159 (1996) 107–111.
[16] Y. Liu, H.T. Zheng, J.R. Liu, T. Zhang, Preparation of high surface area $La_{1-x}A_xMnO_3$ (A = Ba, Sr or Ca) ultra-fine particles used for CH_4 oxidation, Chemical Engineering Journal 89 (2002) 213–221.
[17] A. Dutta, J. Mukhopadhyay, R.N. Basu, Combustion synthesis and characterization of LSCF-based materials as cathode of intermediate temperature solid oxide fuel cells, Journal of the European Ceramic Society 29 (2009) 2003–2011.
[18] S. Shukla, S. Seal, R. Vij, S. Bandyopadhyay, Reduced activation energy for grain growth in nanocrystalline yttria-stabilized zirconia, Nano Letters 3 (2003) 397–401.
[19] X. Ding, C. Cui, L. Guo, Thermal expansion and electrochemical performance of $La_{0.7}Sr_{0.3}CuO_{3-\delta}$–$Sm_{0.2}Ce_{0.8}O_{2-\delta}$ composite cathode for IT-SOFCs, Journal of Alloys and Compounds 481 (2009) 845–850.
[20] R.N. Basu, A.D. Sharma, A. Dutta, J. Mukhopadhyay, Processing of high-performance anode-supported planar solid oxide fuel cell, International Journal of Hydrogen Energy 33 (2008) 5748–5754.
[21] J. Van Herle, R. Ihringer, R. Vasquez Cavieres, L. Constantin, O. Bucheli, Anode supported solid oxide fuel cells with screen-printed cathodes, Journal of the European Ceramic Society 21 (2001) 1855–1859.
[22] M. Zhang, M. Yang, Z. Hou, Y. Dong, M. Cheng, A bi-layered composite cathode of $La_{0.8}Sr_{0.2}MnO_3$-YSZ and $La_{0.8}Sr_{0.2}MnO_3$–$La_{0.4}Ce_{0.6}O_{1.8}$ for IT-SOFCs, Electrochimica Acta 53 (2008) 4998–5006.
[23] C. Jin, J. Liu, W. Guo, Y. Zhang, Electrochemical characteristics of an $La_{0.6}Sr_{0.4}Co_{0.2}Fe_{0.8}O_{3-\delta}$–$La_{0.8}Sr_{0.2}MnO_3$ multi-layer composite cathode for intermediate-temperature solid oxide fuel cells, Journal of Power Sources 183 (2008) 506–511.
[24] S.F. Wang, T. Wang, C. Yeh, Y. Hsu, S. Chyou, W. Lee, Effects of bi-layer $La_{0.6}Sr_{0.4}Co_{0.2}Fe_{0.8}O_3$-based cathodes on characteristics of intermediate temperature solid oxide fuel cells, Journal of Power Sources 196 (2011) 977–987.
[25] J.H. Kim, Y.M. Park, H. Kim, Nano-structured cathodes based on $La_{0.6}Sr_{0.4}Co_{0.2}Fe_{0.8}O_{3-\delta}$ for solid oxide fuel cells, Journal of Power Sources 196 (2011) 3544–3547.
[26] R. Barfod, M. Mogensen, T. Klemensø, A. Hagen, Y. Liu, P.V. Hendriksen, Detailed characterization of anode-supported SOFCs by impedance spectroscopy, Journal of the Electrochemical Society 154 (4) (2007) B371–B378.
[27] A. Leonide, V. Sonn, A. Weber, E. Ivers-Tiffée, Evaluation and modeling of the cell resistance in anode-supported solid oxide fuel cells, Journal of the Electrochemical Society 155 (2008) B36–B41.
[28] A. Leonide, B. Rüger, A. Weber, W.A. Meulenberg, E. Ivers-Tiffée, Impedance study of alternative $LaSrFeO_{3-\delta}$ and $LaSrCoFeO_{3-\delta}$ MIEC cathode compositions, Journal of the Electrochemical Society 157 (2) (2010) B234–B239.
[29] H. Schichlein, A.C. Muller, M. Voigts, A. Krugel, E. Ivers-tiffee, Deconvolution of electrochemical impedance spectra for the identification of electrode reaction mechanisms in solid oxide fuel cells, Journal of Applied Electrochemistry 32 (2002) 875–882.